Chloroquine Inhibits Deferoxamine−induced Ferritinophagy and Potentiates The Cytotoxicity of Chemotherapy Drugs in Lung Cancer Cells[*]

WANG Yong-Wei[1,2)], XIAO Min[1,2)], ZHANG Yu[1,2)], HUO Yan-Wu[1)], WEI Tao-Tao[1,2)**]

([1)]*National Laboratory of Biomacromolecules, Institute of Biophysics, Chinese Academy of Sciences, Beijing 100101, China;*
[2)]*University of Chinese Academy of Sciences, Beijing 100049, China)*

Abstract **Objective** Lung cancer is one of the most commonly diagnosed cancers and the leading cause of cancer deaths worldwide. Despite significant advancements in combined therapy, the numbers of lung cancer cases and deaths continue to rise. Thus, novel therapeutic strategies are necessary to improve cure rates. **Methods** The effect of concomitant use of deferoxamine and chloroquine with frontline chemotherapy drugs was evaluated in lung cancer cells. The autophagy-dependent degradation of ferritin (i.e. ferritinophagy) was determined by western blot and immunofluorescence. The cell proliferation was quantified by cell member and cell cycle. The mitochondrial oxidative phosphorylation was determined by measuring the cellular oxygen consumption. **Results** The iron chelator deferoxamine induced ferritinophagy in cancer cells, and this process was blocked by chloroquine, an anti-malaria drug. Exposure of lung cancer cells to deferoxamine and chloroquine together inhibited mitochondrial oxidative phosphorylation, caused the accumulation of G1 phase cells and blocked cell proliferation. More importantly, the use of deferoxamine and chloroquine concomitantly with cisplatin or etoposide resulted in a significant increase in cytotoxicity in lung cancer cells when compared with the same concentration of cisplatin or etoposide alone. **Conclusion** These data indicate the efficacy of targeting ferritinophagy for the sensitization of iron-addicted cancer cells to chemotherapy, and introduce a potential targeted therapeutic approach for the treatment of cancer.

Lung cancer is the most commonly diagnosed cancer worldwide[1], comprising 13% new cancer cases in males and 12% in females[2]. As lung cancer may remain asymptomatic and lacks early symptoms and is discovered at advanced stages[3], its mortality remains high, comprising 23% cancer-related deaths in males and 22% in females[2, 4]. The five-year survival rate of lung cancer various from 4%−17% in patients based on the stage and regional differences[5]. Strategies to treat lung cancer mainly include surgery, chemotherapy, radiation therapy and immunotherapy[5-6]. In spite of the significant advancement in combined therapy, the numbers of lung cancer cases and deaths continue to rise[7]. Only a fraction of patients derive benefit from the immune checkpoint inhibitors[8], and the chemotherapy just slightly prolongs the survival among the advanced disease, due to drug resistance and side effects. Thus, novel therapeutic strategies are necessary to improve cure rates.

Iron is a bio-trace element essential for cell survival and cell proliferation. Compared with normal cells, cancer cells grow rapidly and uncontrolledly, and show a stronger dependence on iron. Cancer cells

---

often exhibit high rate of iron metabolism, with increased transferrin receptor 1 (TfR1) and LCN2 receptor (LCN2R), and down-regulated ferroportin 1[9]. Elevated iron level increases cancer incidence and contributes to tumor growth and progression[10-12]. Therefore, targeting iron transportation and metabolism in cancer cells might be used as a potential target for cancer therapy[13-14].

Iron ions transported into cells initially enter a dynamic, exchangeable pool known as labile iron pool (LIP)[15-16], and can be deprived by iron chelators[17]. The majority of the iron in LIP can directly be incorporated into cofactors such as heme and iron-sulfur clusters[18]. To avoid the generation of reactive oxygen species (ROS), excessive iron is stored in the form of ferritin[19]. When more iron is needed, ferritin could be degraded *via* an autophagic pathway, referred to as ferritinophagy[20-22], by which the stored iron is released for utilization. Studies have revealed that the C-terminal conserved domain of NCOA4 directly interacts with the ferritin heavy chain (FTH1), thus mediates the ferritinophagy under iron deficiency conditions. Under high iron conditions, NCOA4 is degraded *via* the iron-dependent E3 ubiquitin ligase HERC2[20-21]. Thus, targeting NCOA4-dependent iron regulation might be an effective approach to combat iron-addicted cancer cells.

We hereby provide direct evidence that chloroquine (CQ), a drug long been used to treat or prevent malaria, blocked the deferoxamine (DFO) - induced, NCOA4-dependent, and autophagy-mediated degradation of ferritin (*i. e.* ferritinophagy). Concomitant exposure of cancer cells to DFO and CQ inhibited mitochondrial oxidative phosphorylation, caused the accumulation of G1 phase cells, blocked cell proliferation, and potentiated the cytotoxicity of cisplatin and etoposide in lung cancer cells.

1　Materials and methods

1.1　Materials

DFO and MG132 were purchased from Sigma-Aldrich (St. Louis, MO, USA). Bafilomycin-A1 (Baf-A1) and chloroquine phosphate (CQ) were from MedChemExpress (Monmouth Junction, NJ, USA). 5-Bromo-2'-deoxyuridine (BrdU) was from Sangon (Shanghai, China). Pierce[TM] BCA protein assay kit

was from Thermo Fisher (Beijing, China). Cell Counting Kit-8 (CCK-8) and Cell Cycle/Apoptosis kit were from Yeasen (Shanghai, China).

Antibodies against FTH1 (ab75972) and NCOA4 (ab86707) were from Abcam (Cambridge, UK). Antibodies against LC3 (2775) and BrdU (5292) were form CST (Danvers, MA, USA). Antibodies against FTL (10727-1-AP), Cyclin D1 (60186-1-AP), CDK4 (11026-1-AP) and CDK6 (14052-1-AP) were from Proteintech (Rosemont, USA). Antibody against β-actin (D191047) was from Sangon (Shanghai, China). Antibody against P62 (PM045) was from MBL (Tokyo, Japan). Horseradish peroxidase (HRP)-conjugated and Alexa Fluor ®488-conjugated secondary antibodies were from Zhongshan Golden Bridge (Beijing, China).

1.2　Cell culture

Human cervical cancer cell line HeLa, human non-small cell lung cancer cell lines A549 and NCI-H1299 were obtained from the American Type Culture Collection (ATCC). HeLa and NCI-H1299 cells were grown in DMEM, and A549 cells were cultured in F12K medium, supplemented with 10% fetal bovine serum in a humidified atmosphere of 5% CO_2 at 37℃.

1.3　Immunoblot

Cells were washed by precooled phosphate buffer solution (PBS) and total cell protein was extracted by RIPA buffer. Immunoblot analysis was performed as described previously[23]. The expression profiles of the proteins were visualized by enhanced chemiluminescence.

1.4　Immunofluorescence

Cells cultured on glass coverslips were treated with DFO and/or CQ for 10 h, fixed with 4% paraformaldehyde, permeabilized with 0.2% Triton X-100, and blocked with 5% BSA. Then cells were incubated with rabbit anti-LC3 primary antibody (1∶200) at 4℃ overnight, washed with PBS, and incubated with Alexa Fluor ®488-conjugated secondary antibody (1∶200) for 1 h. The nuclei were stained by DAPI. The cells were viewed with an Olympus FV1200 laser confocal scanning microscope.

1.5　Mitochondrial oxidative phosphorylation assay

Oxidative phosphorylation (OXPHOS) was

measured with a Seahorse XF-24 extracellular analyzer as described previously[23]. Cells were seeded into a Seahorse XF-24 analyzer cell culture plate and treated with DFO (10 μmol/L) and/or CQ (10 μmol/L) for 24 h. The oxygen consumption rate (OCR) was detected based on the standard Mito-stress assay protocol.

1.6　Cell proliferation assays

Cells were seeded into 6-well plates and treated with DFO and/or CQ for 48 h. Then the cells were fixed with 4% paraformaldehyde and stained with 0.1% crystal violet. The cell intensity was analyzed by ImageJ software.

For quantification of cell proliferation, cells were seeded into 24-well plates and treated with DFO and/ or CQ for 24, 48 and 72 h. The number of viable cells was counted with an automated cell counter (Countstar).

For BrdU incorporation assay, cells were treated with DFO and CQ for 36 h and then incubated with BrdU (30 mg/L) for 30 min. Then cells were harvested, fixed with precooled 70% ethanol, and permeabilized with 1.5 mol/L HCl. Cells were then incubated with anti-BrdU primary antibody (1∶200) and Alexa Fluor ®488-conjugated secondary antibody (1∶200). The percentage of BrdU-positive cells was quantified by BD FACScalibur flow cytometry.

1.7　Analysis of cell cycle

The cell cycle was analyzed by flow cytometry[24]. Briefly, cells were treated with DFO and/or CQ for 18 h. Then cells were collected and fixed with precooled 70% ethanol overnight, treated with RNAse A, stained with PI, and analyzed by BD FACSCalibur flow cytometry.

1.8　Determination of cell viability

The cell viability was quantified by CCK-8 kit following protocols we described previously[25]. Briefly, cells cultured in 96-well plates were treated with indicated concentrations of DFO, CQ, cisplatin or etoposide for 48 h. Then the cells were incubated with CCK-8 reagent for 2 h and the OD at 450 nm was measured.

1.9　Statistical analysis

All experiments were repeated for at least three times. The differences were analyzed by two-side Student's t-tests between groups. The statistically significant difference was indicated as *$P < 0.05$, **$P < 0.01$ and ***$P < 0.001$.

2　Results

2.1　Chloroquine inhibits deferoxamine−induced ferritin degradation *via* the blockade of autophagy

DFO chelated and depleted extracellular free iron ions, and induced the degradation of ferritin, as evidenced by the decrease of ferritin heavy chain (FTH1), ferritin light chain (FTL), and ferritin adaptor protein NCOA4 (Figure 1a). Baf-A1 and CQ, two compounds known to inhibit autophagic flux, blocked DFO-induced degradation of P62, FTH1, FTL and NCOA4. On the contrary, MG132, an inhibitor of proteasomes, showed no effect on ferritin degradation. CQ also inhibited P62 and ferritin degradation in A549 and NCI-H1299 lung cancer cells (Figure 1b), suggesting that the DFO-induced ferritin degradation depend on the autophagic pathway in different cancer cells.

To further confirm the involvement of autophagy in DFO-induced ferritin degradation (termed as ferritinophagy), we observed the intracellular localization of LC3. DFO treatment caused the accumulation of LC3 puncta within cells (Figure 1c), suggesting the elevated levels of autophagy. CQ elevated LC3 level and increased the numbers of LC3 puncta, suggesting that CQ blocked DFO-induced autophagic flux effectively.

2.2　Deferoxamine and chloroquine inhibits mitochondrial oxidative phosphorylation

Iron is crucial for the mitochondrial electron transfer chain complexes and thus plays key roles in the maintenance of mitochondrial oxidative phosphorylation[26]. Given the fact that CQ inhibited DFO-induced ferritinophagy and interfered the release of stored iron in cancer cells, we determined the impact of DFO and CQ on mitochondrial oxidative phosphorylation. NCI-H1299 cells were incubated with DFO (10 μmol/L) in the presence or absence of CQ (10 μmol/L) for 24 h, and the OCR (an index of mitochondrial oxidative phosphorylation capacity) was monitored at real time. Results shown in Figure 2 indicated that DFO or CQ showed no apparent effects
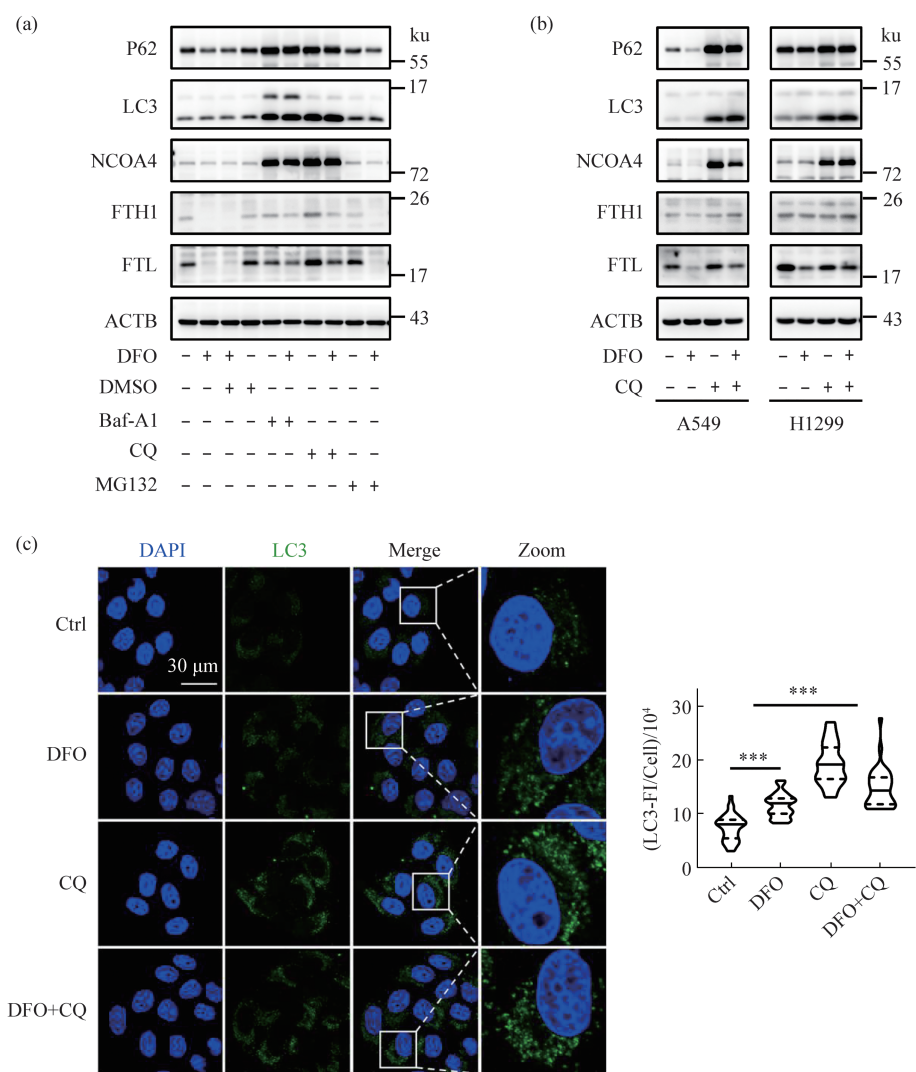
Fig. 1　Chloroquine inhibits deferoxamine−induced ferritin degradation

(a) HeLa cells were treated with deferoxamine (DFO; 100 μmol/L) in the presence or absence of Bafimycin-A1 (Baf-A1; 50 nmol/L), chloroquine phosphate (CQ; 20 μmol/L) and MG132 (5 μmol/L) for 24 h. (b) A549 and NCI-H1299 cells were treated with DFO and/or CQ for 24 h. (c) HeLa cells were treated with DFO and/or CQ for 10 h, and the intracellular localization of LC3 was observed by immunofluorescence. For quantification of intracellular LC3 puncta, more than 30 randomly selected cells per coverslip were analyzed. ***, $P < 0.001$ compared with control.

on the basal and maximal OCR in NCI-H1299 cells. However, when cells were treated with DFO and CQ concomitantly, the OCR was inhibited markedly. In comparison with control cells, the basal OCR was decreased by $(26.9 \pm 1.3)\%$, the maximal OCR was decreased by $(33.9 \pm 6.7)\%$, and the ATP-generation coupled OCR was decreased by $(28.2 \pm 5.9)\%$ in cells treated with DFO and CQ concomitantly. These results indicated a synergistic inhibition of mitochondrial oxidative phosphorylation by DFO and CQ.
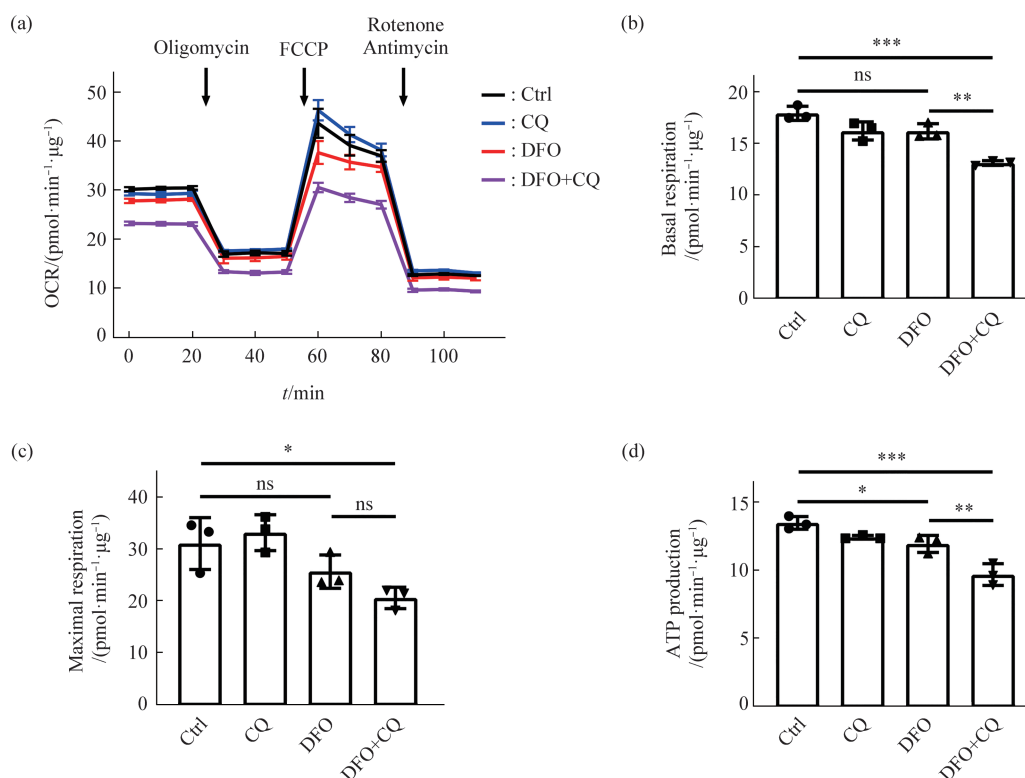
Fig. 2 Deferoxamine and chloroquine inhibits mitochondrial oxidative phosphorylation

(a) NCI-H1299 cells were treated with DFO (10 μmol/L) and/or CQ (10 μmol/L) for 24 h, and then the oxygen consumption rate (OCR) was monitored with the Seahorse XF24-3 extracellular analyzer. The basal (b), maximal (c) and ATP production-coupled (d) OCR was calculated from Figure 2a. The data were shown as $\bar{x} \pm s$ of three independent experiments. *, $P < 0.05$; **, $P < 0.01$; ***, $P < 0.001$ compared with control.

2.3 Deferoxamine and chloroquine suppresses cell proliferation

We evaluated the influence of DFO and CQ on cell proliferation. A549 cells and NCI-H1299 cells were incubated with DFO (20 μmol/L for A549 and 10 μmol/L for NCI-H1299) in the presence or absence of CQ (20 μmol/L for A549 and 10 μmol/L for NCI-H1299) for 48 h, then cells were stained with crystal violet, and the number of cells was estimated. Results shown in Figure 3a and 3b clearly indicated that DFO exposure caused a significant growth retardation in both A549 cells and NCI-H1299 cells, and the concomitant addition of CQ further inhibited the growth of cells. Next, we quantified the impact of DFO and/or CQ on the growth of lung cancer cells.

The number of cells was counted 24, 48 and 72 h after seeding with an automated cell counter. The results shown in Figure 3c and 3d indicated that the number of cells remained unchanged in cells exposed to DFO and CQ concomitantly, suggesting the significant suppression of cell proliferation.

To further confirm the suppression of cell proliferation by DFO and CQ, we analyzed the DNA replication in cancer cells by BrdU incorporation assay[27-28]. As shown in Figure 3e and 3f, the percentage of BrdU-positive cells was (50.8±3.6)% (A549) and (49.8±1.7)% (NCI-H1299) in control cultures, respectively. After DFO and CQ treatment, the percentage of BrdU-positives cells decreased to (27.4±4.6)% (A549) and (22.1±2.7)% (NCI-H1299).
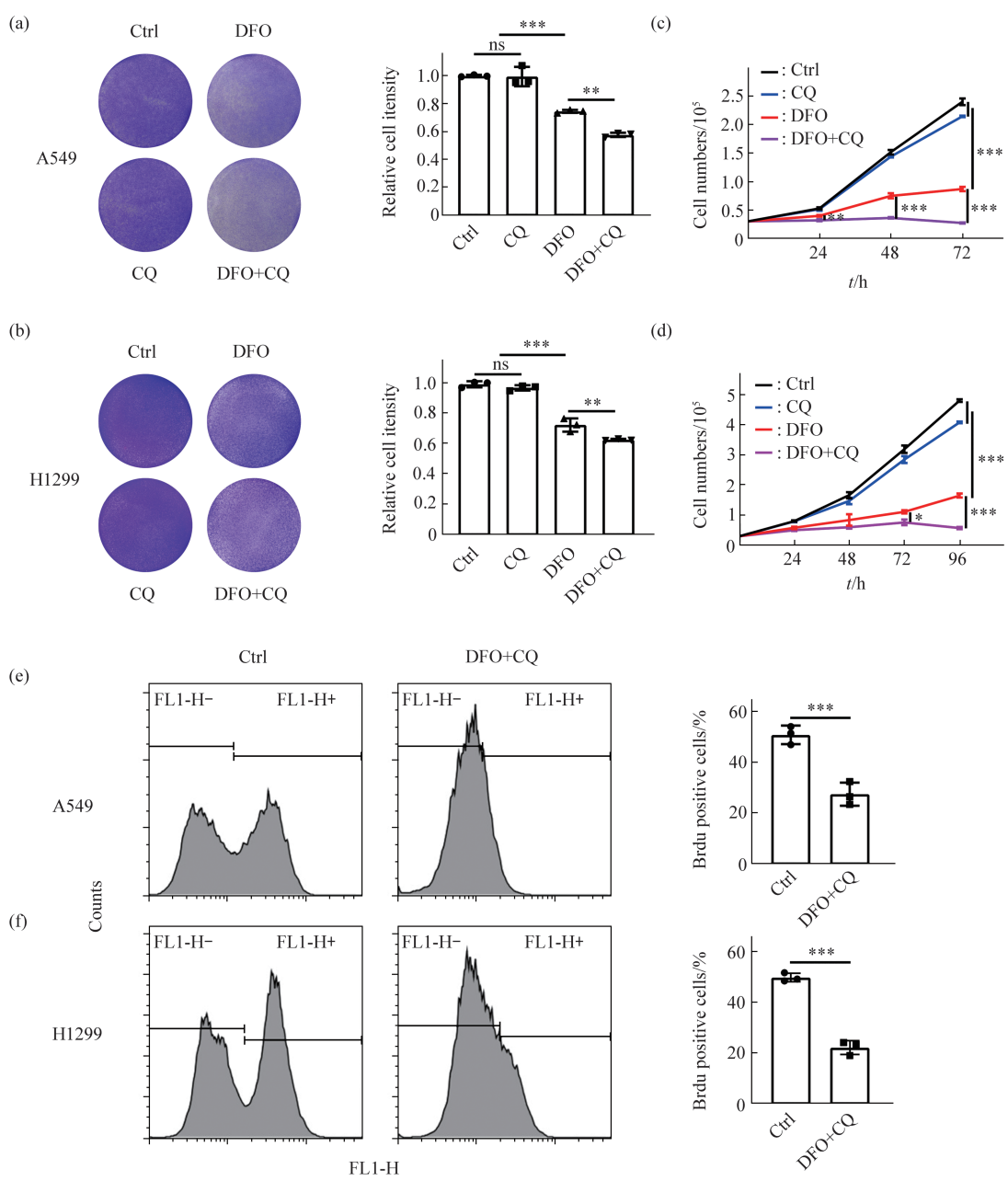
Fig. 3 Deferoxamine and chloroquine suppresses cell proliferation

A549 (a) and NCI-H1299 (b) cells were treated with DFO (A549, 20 μmol/L; H1299 10 μmol/L) and/or CQ (A549, 20 μmol/L, H1299 10 μmol/L) for 48 h, stained with crystal violet, and the number of cells was estimated by ImageJ software. A549 (c) and NCI-H1299 (d) cells were treated with DFO and/or CQ for 24, 48, 72, 96 h, and quantified with an automated cell counter. A549 (e) and NCI-H1299 (f) cells were treated with DFO and/or CQ for 36 h, labeled with BrdU, and the percentage of BrdU-incorporated cells was determined by flow cytometry. The data were shown as $\bar{x} \pm s$ of three independent experiments. *, $P < 0.05$; **, $P < 0.01$; ***, $P < 0.001$ compared with control.

2.4 Deferoxamine and chloroquine induces cell cycle arrest

Since DFO and CQ suppressed cell proliferation significantly in lung cancer cells, we analyzed their impact on cell cycle. Flow cytometry analysis indicated that the percentage of G1 phase cells was (62.4±0.6)% (A549) and (55.4±0.3)% (NCI-H1299) in untreated cells, respectively. Upon DFO and CQ

treatment, the percentage of G1 phase cells increased to (81.3±0.1)% (A549) and (71.6±1.0)% (NCI-H1299), as shown in Figure 4a and 4b. Immunoblot analysis indicated that DFO and CQ decreased the levels of G1/S phase-associated cyclin D1, CDK4 and CDK6 (Figure 4c), suggesting that DFO and CQ exposure caused the cell cycle arrest in cancer cells.

2.5 Deferoxamine and chloroquine potentiates the cytotoxicity of cisplatin and etoposide

The above data demonstrated that CQ blocked DFO-induced ferritin degradation, inhibited mitochondrial OXPHOS, induced cell cycle arrest, and suppressed the proliferation of lung cancer cells. Next, we evaluated the impact of DFO and CQ on the cytotoxicity of chemotherapy drugs. Cisplatin and etoposide, two frontline drugs used for the

chemotherapy of lung cancer, induced cell death in both A549 and NCI-H1299 cells. In cells treated with 10 μmol/L cisplatin for 48 h, the relative viability was (76.59±1.30)% (A549) and (83.91±1.07)% (NCI-H1299). DFO and CQ further potentiated the cytotoxicity of cisplatin (Figure 5a). In A549 cells treated with 10 μmol/L cisplatin, 16 μmol/L DFO and 10 μmol/L CQ for 48 h, the relative viability was (36.93±0.96)% . In NCI-H1299 cells treated with 10 μmol/L cisplatin, 16 μmol/L DFO and 10 μmol/L CQ for 48 h, the relative viability was (49.48±1.57)%. The cytotoxicity of etoposide could also be potentiated by DFO and CQ (Figure 5b), suggesting that DFO and CQ increased the sensibility to cisplatin or etoposide in lung cancer cells *in vitro*.
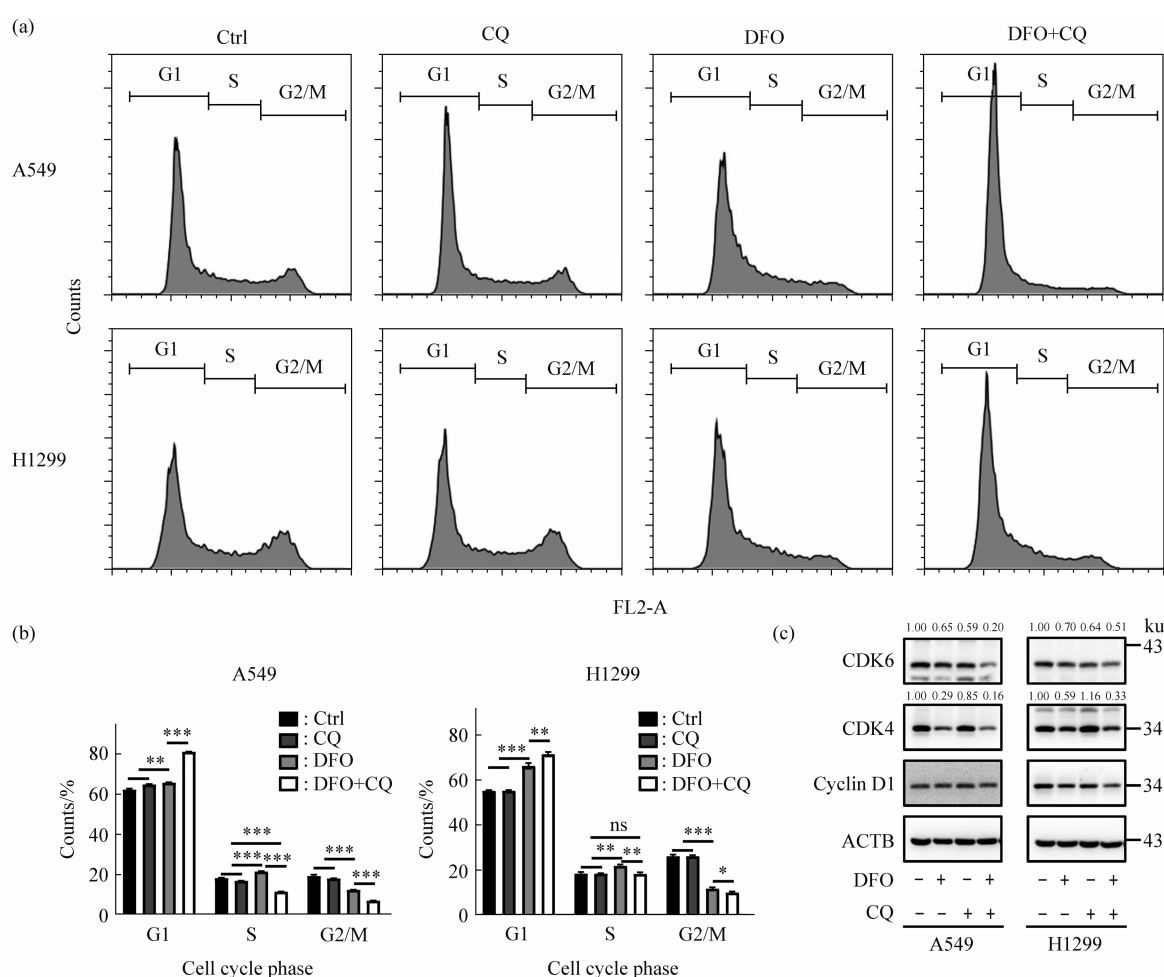

Fig. 4 Deferoxamine and chloroquine causes cell cycle arrest

A549 (a) and NCI-H1299 (b) cells were treated with DFO (A549, 20 μmol/L; H1299 10 μmol/L) and/or CQ (A549, 20 μmol/L; H1299 10 μmol/L) for 18 h, and the cell cycle was analyzed by flow cytometry. (c) A549 and NCI-H1299 cells were treated with DFO and/or CQ for 24 h, and the levels of cell cycle-related proteins cyclin D1, CDK4 and CDK6 were analyzed by immunoblot. The ratio of CDK/β-actin was calculated with ImageJ. The data were shown as $\bar{x} \pm s$ of three replicates. *, $P < 0.05$；**, $P < 0.01$；***, $P < 0.001$ compared with control.
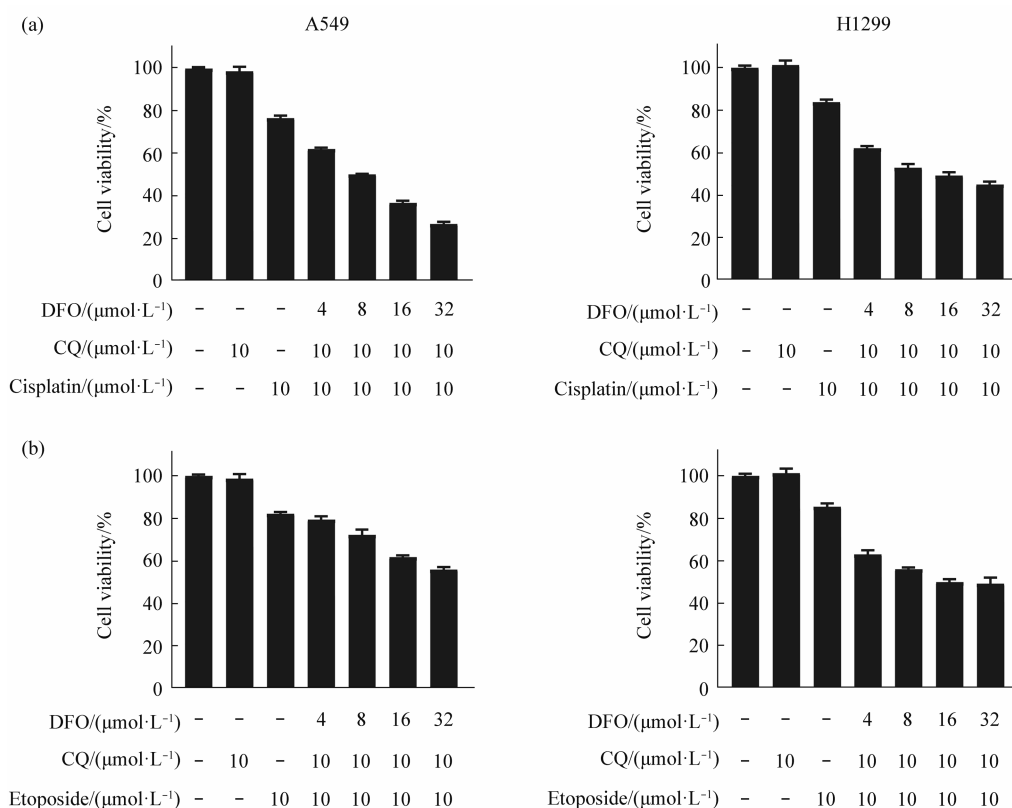
Fig. 5 Deferoxamine and chloroquine potentiates the sensibility to cisplatin or etoposide

A549 and NCI-H1299 cells were treated with indicated concentrations of DFO, CQ, cisplatin(a) and/or etoposide(b) for 48 h. The cell viability was detected by CCK-8 assay. The data were shown as $\bar{x} \pm s$ of six replicates.

3 Discussion

Autophagy is an evolutionarily conserved adaptive process that occurs in response to different forms of stress, including nutrient deprivation, growth factor depletion, and infection[29], with its main function to provide nutrients for vital cellular functions *via* lysosome-associated breaking down of macromolecules[30-31]. Autophagy also selectively eliminates unwanted, potentially harmful cytosolic material, such as damaged organelles or protein aggregates, and thus modulates many pathologies, including neurodegeneration, infectious diseases and cancer[32]. There is growing evidence that autophagy can help cope with intracellular and environmental stresses, such as hypoxia, nutrient shortage, or drug treatment, thereby favoring tumor progression[33]. Accordingly, autophagy inhibition could improve therapeutic outcomes for patients with advanced cancer[34]. Among the many inhibitors for autophagy, CQ, a drug long been used to treat or prevent malaria,

attracted much more attention. Several clinical trials that have been conducted or are in progress have shown favorable effects of CQ as novel antitumor drug[35-36]; however, effective repurposing of existing CQ derivatives for cancer has been limited by a missing molecular target[33]. Thus, targeting specific autophagic pathways might improve the anticancer effects of autophagy inhibitors.

Compared with non-cancerous epithelial cells, lung cancer cells are characterized by rapid proliferation and vigorous metabolism, which are empowered by a higher requirement for iron[37-39]. For example, Fe-S clusters and heme are essential cofactors for the electron transfer within the mitochondria. Enzymes responsible for DNA synthesis and repair, such as ribonucleotide reductase and DNA helicases, also contain iron as cofactors[40]. Recently, it has been documented that NCOA4 mediates the autophagic degradation of ferritin (*i. e.* ferritinophagy), which plays essential roles in the maintenance of cellular iron hemostasis by facilitating

ferritin iron storage or release according to demand[41]. Thus, we selected ferritinophagy as the potential target of CQ, and investigated the effects of CQ on the energy metabolism, proliferation, and cell death in lung cancer cells.

We start our investigation by treating cancer cells with DFO, an FDA-approved iron chelator for the treatment of acute and chronic iron overload in clinic[42]. DFO chelated extracellular iron[43], and caused the blockage of iron absorption. Prolonged exposure of cancer cells to DFO depleted the intracellular LIP[20-22], and triggered the ferritinophagy, by which iron was released from ferritin. CQ inhibited DFO-induced ferritinophagy effectively, as evidenced by the blockade of degradation of ferritin and NCOA4. The inhibition of ferritinophagy by CQ decreased mitochondrial oxidative phosphorylation, induced cell cycle arrest, suppressed cell proliferation, and potentiated the cytotoxicity of frontline chemotherapy drugs cisplatin and etoposide.

Our data suggested that DFO, an FDA-approved drug for iron overload, in combination with CQ, an FDA-approved drug for malaria, potentiated the efficacy of two chemotherapy drugs *in vitro*. However, there are still some issues to be addressed before *in vivo* experiments and clinical trials. The limitation of DFO application in clinic is the very short plasma half-life[44] *in vivo*. We hypothesized that a cancer tissue-targeted, nanomedicine-based drug carrier for DFO and CQ co-delivery might be a promising strategy to solve these problems.

References

[1] Bray F, Ferlay J, Soerjomataram I, *et al*. Global cancer statistics 2018: GLOBOCAN estimates of incidence and mortality worldwide for 36 cancers in 185 countries. CA Cancer J Clin, 2018, **68**(6): 394-424

[2] Siegel R L, Miller K D, Jemal A. Cancer statistics, 2020. CA Cancer J Clin, 2020, **70**(1): 7-30

[3] Nasim F, Sabath B F, Eapen G A. Lung cancer. Med Clin North Am, 2019, **103**(3): 463-473

[4] Chen W, Zheng R, Baade P D, *et al*. Cancer statistics in China, 2015. CA Cancer J Clin, 2016, **66**(2): 115-132

[5] Hirsch F R, Scagliotti G V, Mulshine J L, *et al*. Lung cancer: current therapies and new targeted treatments. Lancet, 2017, **389**(10066): 299-311

[6] Steven A, Fisher S A, Robinson B W. Immunotherapy for lung cancer. Respirology, 2016, **21**(5): 821-833

[7] Bade B C, Dela Cruz C S. Lung cancer 2020: epidemiology, etiology, and prevention. Clin Chest Med, 2020, **41**(1): 1-24

[8] Goff P H, Zeng J, Rengan R, *et al*. Radiation and modulation of the tumor immune microenvironment in non-small cell lung cancer. Semin Radiat Oncol, 2021, **31**(2): 133-139

[9] Torti S V, Torti F M. Iron and cancer: more ore to be mined. Nat Rev Cancer, 2013, **13**(5): 342-355

[10] Manz D H, Blanchette N L, Paul B T, *et al*. Iron and cancer: recent insights. Ann N Y Acad Sci, 2016, **1368**(1): 149-161

[11] Torti S V, Manz D H, Paul B T, *et al*. Iron and cancer. Annu Rev Nutr, 2018, **38**: 97-125

[12] Chen Y, Fan Z, Yang Y, *et al*. Iron metabolism and its contribution to cancer (Review). Int J Oncol, 2019, **54**(4): 1143-1154

[13] Lui G Y, Obeidy P, Ford S J, *et al*. The iron chelator, deferasirox, as a novel strategy for cancer treatment: oral activity against human lung tumor xenografts and molecular mechanism of action. Mol Pharmacol, 2013, **83**(1): 179-190

[14] Corce V, Gouin S G, Renaud S, *et al*. Recent advances in cancer treatment by iron chelators. Bioorg Med Chem Lett, 2016, **26**(2): 251-256

[15] Kakhlon O, Cabantchik Z I. The labile iron pool: characterization, measurement, and participation in cellular processes. Free Radic Biol Med, 2002, **33**(8): 1037-1046

[16] Camaschella C, Pagani A. Advances in understanding iron metabolism and its crosstalk with erythropoiesis. Br J Haematol, 2018, **182**(4): 481-494

[17] Glickstein H, Ben El R, Shvartsman M, *et al*. Intracellular labile iron pools as direct targets of iron chelators: a fluorescence study of chelator action in living cells. Blood, 2005, **106**(9): 3242-3250

[18] Hentze M W, Muckenthaler M U, Galy B, *et al*. Two to tango: regulation of Mammalian iron metabolism. Cell, 2010, **142**(1): 24-38

[19] Arosio P, Ingrassia R, Cavadini P. Ferritins: a family of molecules for iron storage, antioxidation and more. BBA-Gen Subjects, 2009, **1790**(7): 589-599

[20] Mancias J D, Vaites L P, Nissim S, *et al*. Ferritinophagy *via* NCOA4 is required for erythropoiesis and is regulated by iron dependent HERC2-mediated proteolysis. Elife, 2015, **4**: e10308

[21] Mancias J D, Wang X X, Gygi S P, *et al*. Quantitative proteomics identifies NCOA4 as the cargo receptor mediating ferritinophagy. Nature, 2014, **509**(7498): 105-109

[22] Goodall M, Thorburn A. Identifying specific receptors for cargo-mediated autophagy. Cell Res, 2014, **24**(7): 783-784

[23] Zhao L, Zhao X, Zhao K, *et al*. The alpha-tocopherol derivative ESeroS-GS induces cell death and inhibits cell motility of breast cancer cells through the regulation of energy metabolism. Eur J

Pharmacol, 2014, **745**: 98-107

[24] 化朝举, 戴斐, 邓瑶, 等 . EF4影响线粒体氧化磷酸化并调控膀胱癌细胞增殖及迁移 . 生物化学与生物物理进展, 2021, **48**(3): 317-327
Hua C J, Dai F, Deng Y, *et al*. Prog Biochem Biophys, 2021, **48**(3): 317-327

[25] Zhang J, Yan L, Wei P, *et al*. PEG-GO@XN nanocomposite suppresses breast cancer metastasis *via* inhibition of mitochondrial oxidative phosphorylation and blockade of epithelial-to-mesenchymal transition. Eur J Pharmacol, 2021, **895**: 173866

[26] Paul B T, Manz D H, Torti F M, *et al*. Mitochondria and iron: current questions. Expert Rev Hematol, 2017, **10**(1): 65-79

[27] Li S, Zhang Y, Wang N, *et al*. Pan-cancer analysis reveals synergistic effects of CDK4/6i and PARPi combination treatment in RB-proficient and RB-deficient breast cancer cells. Cell Death Dis, 2020, **11**(4): 219

[28] Dean J L, McClendon A K, Knudsen E S. Modification of the DNA damage response by therapeutic CDK4/6 inhibition. J Biol Chem, 2012, **287**(34): 29075-29087

[29] Gonzalez A, Hall M N, Lin S C, *et al*. AMPK and TOR: the Yin and Yang of cellular nutrient sensing and growth control. Cell Metab, 2020, **31**(3): 472-492

[30] Kroemer G, Marino G, Levine B. Autophagy and the integrated stress response. Mol Cell, 2010, **40**(2): 280-293

[31] Kim K H, Lee M S. Autophagy--a key player in cellular and body metabolism. Nat Rev Endocrinol, 2014, **10**(6): 322-337

[32] Dikic I, Elazar Z. Mechanism and medical implications of mammalian autophagy. Nat Rev Mol Cell Biol, 2018, **19**(6): 349-364

[33] Amaravadi R K, Kimmelman A C, Debnath J. Targeting autophagy in cancer: recent advances and future directions. Cancer Discov, 2019, **9**(9): 1167-1181

[34] Galluzzi L, Bravo-San Pedro J M, Levine B, *et al*. Pharmacological modulation of autophagy: therapeutic potential and persisting obstacles. Nat Rev Drug Discov, 2017, **16**(7): 487-511

[35] Yang Z J, Chee C E, Huang S, *et al*. The role of autophagy in cancer: therapeutic implications. Mol Cancer Ther, 2011, **10**(9): 1533-1541

[36] Kimura T, Takabatake Y, Takahashi A, *et al*. Chloroquine in cancer therapy: a double-edged sword of autophagy. Cancer Res, 2013, **73**(1): 3-7

[37] Devireddy L R, Gazin C, Zhu X, *et al*. A cell-surface receptor for lipocalin 24p3 selectively mediates apoptosis and iron uptake. Cell, 2005, **123**(7): 1293-1305

[38] Wang B, Zhang J, Song F, *et al*. EGFR regulates iron homeostasis to promote cancer growth through redistribution of transferrin receptor 1. Cancer Lett, 2016, **381**(2): 331-340

[39] Sun B B, Guo W Z, Hu S, *et al*. Gprc5a-knockout mouse lung epithelial cells predicts ceruloplasmin, lipocalin 2 and periostin as potential biomarkers at early stages of lung tumorigenesis. Oncotarget, 2017, **8**(8): 13532-13544

[40] Puig S, Ramos-Alonso L, Romero A M, *et al*. The elemental role of iron in DNA synthesis and repair. Metallomics, 2017, **9**(11): 1483-1500

[41] Santana-Codina N, Mancias J D. The role of NCOA4-mediated ferritinophagy in health and disease. Pharmaceuticals (Basel), 2018, **11**(4): 114

[42] Kontoghiorghe C N, Kontoghiorghes G J. Efficacy and safety of iron-chelation therapy with deferoxamine, deferiprone, and deferasirox for the treatment of iron-loaded patients with non-transfusion-dependent thalassemia syndromes. Drug Des Devel Ther, 2016, **10**: 465-481

[43] Porter J B, Rafique R, Srichairatanakool S, *et al*. Recent insights into interactions of deferoxamine with cellular and plasma iron pools: implications for clinical use. Ann Ny Acad Sci, 2005, **1054**: 155-168

[44] Sheth S. Iron chelation: an update. Curr Opin Hematol, 2014, **21**(3): 179-185

氯喹抑制铁蛋白自噬并增强肺癌细胞对化疗药物敏感性的研究[*]

王永伟[1,2]　肖　敏[2]　张　瑀[1,2]　霍艳武[1]　卫涛涛[1,2][**]

（[1] 中国科学院生物物理研究所，生物大分子国家重点实验室，北京 100101；

[2] 中国科学院大学，北京 100049）

摘要　目的　肺癌的发病率和致死率高居世界恶性肿瘤首位。尽管肺癌的诊断与治疗治疗已取得进展，但其发病率和致死率仍呈逐年上升的趋势，因此急需寻找有效的干预靶标和治疗手段。**方法**　本文验证了通过自噬抑制剂干预铁蛋白自噬、增加肺癌细胞对化疗药物敏感性的多药联用策略。通过免疫印迹分析及免疫荧光测定了细胞中铁蛋白的自噬性降解（铁蛋白自噬），通过分析细胞数量及细胞周期测定了细胞增殖，通过分析细胞耗氧速率评估了细胞线粒体氧化磷酸化水平。**结果**　铁螯合剂去铁胺可诱导肿瘤细胞发生铁蛋白自噬；氯喹等自噬抑制剂可有效抑制去铁胺诱导的铁蛋白降解，显著抑制肿瘤细胞线粒体氧化磷酸化，并引发细胞周期阻滞、抑制细胞增殖；去铁胺、氯喹与一线化疗药物顺铂或依托泊苷的联合给药可显著增强化疗药物对肺癌细胞的毒性。**结论**　通过自噬抑制剂和铁螯合剂干预细胞铁代谢有望成为提升肺癌化疗治疗效果的潜在新策略。

关键词　肺癌，铁蛋白自噬，去铁胺，氯喹，化疗

中图分类号　R734.2，Q28　　　　　　　　　　　**DOI**：10.16476/j.pibb.2021.0090